Physics AUC, vol. 32, 88-102 (2022) PHYSICS AUC

Analysis of reactivity control coefficients and the stability of an AP1000 reactor assembly fueled with (Th-^{233}U)O_2 using DRAGON code

Zohair BENRHNIA [1], Ouadie KABACH [1,*], Abdelouahed CHETAINE [1], Abdelmajid SAIDI [1], Hamid AMSIL [2], Abdelfettah BENCHRIF [2], Fadi El BANNI [3]
[1] Nuclear Reactor and Nuclear Security Group, Energy Centre, Department of Physics, FSR, Mohammed V University, Rabat, Morocco
[2] Direction of Studies and Scientific Researches, National Centre of Nuclear Energy Sciences and Techniques (CNESTEN), Rabat, Morocco
[3] New Energies Research Institute, Nangui Abrogoua University, Abidjan, Ivory Coast
*Corresponding author: ouadie.kabach10@gmail.com; ouadie_kabach@um5.ac.ma

Abstract

Reactivity coefficients are essential parameters for a nuclear reactor's inherent safety and stability. The calculation of changes in reactivity caused by changes in the fuel mixture, temperatures, or the addition of a reactivity control method such as burnable absorbers is required to provide the reactor safety analysis because it is related to reactor operation. Recently, the use of (Th-^{233}U)O_2 fuel in commercial nuclear power reactors has been proposed and studied, with the primary goal of using thorium in a sustainable manner. However, such implementation should be accompanied by a thorough comparison with the widely used UO_2 fuel because these fuels have different fissile and fertile nuclei. As a result, the purpose of this research is to simulate the behavior of an assembly fueled by (Th-^{233}U)O_2 on the main reactivity characteristics of a Westinghouse AP1000 advanced passive pressurized water reactor. The assembly calculations for the determination of the reactivity coefficient parameter are done by using deterministic DRAGON5 code. In the first stage, the infinity multiplication factor and the reactivity change with burnup of (Th-^{233}U)O_2 and UO_2 fuels were compared, as well as the temperature and boron worth reactivity coefficients. In the second stage, the effect of ZrB_2, Gd_2O_3, Er_2O_3, or PaO_2 as burnable absorbers, whether homogeneously mixed or coated on (Th-^{233}U)O_2 fuel rods, on the infinity multiplication factor and the reactivity change with burnup, as well as the temperature reactivity coefficients, was investigated to quantify the degree to which these absorbers can achieve acceptable limits.

Keywords: AP1000 assembly, (Th-^{233}U)O_2 fuel, reactivity coefficients, burnable absorbers, reactivity suppression, reactivity swing, inherent safety, DRAGON code

1. Introduction

Given the scarcity of natural uranium resources and a mismatch between uranium production and reactor operation requirements for future needs, thorium has been investigated as an alternative nuclear fuel for use in reactors [1-2]. Thorium is found naturally in the form of Th-232. By absorbing neutrons, Th-232 can be converted into the fissile material U-233. However, because thorium lacks a naturally occurring fissile isotope, it must be combined with a fissile material like U-233, U-235, Pu-239, or Pu-241. Th-232 mixed with one of these fissile isotopes has been thoroughly investigated as a potential replacement for established reactor technologies

such as Generation III water reactors, Generation III+ water reactors, molten salt reactors, and advanced high-temperature reactors [1, 3-5].

According to relevant studies, (Th-^{233}U)O_2 fuel is a practical combination because the ultimate goal is to use thorium in a sustainable manner [6-8], as shown in Figure 1. U-233 alone produces enough neutrons per thermal neutron (the number of fission neutrons released per neutron absorbed) to match or exceed its consumption [7]. In this way, U-233 serves as a catalyst for long-term energy production from Th-232 and can almost completely eliminate transuranic production [9]. However, there is currently very little U-233 available, and not enough for a significant rollout of thorium reactors. Even so, U-233 can be produced in a reactor or accelerator by bombarding Th-232 with neutrons. U-233 can also be recovered from irradiated thorium using chemical separation in a nuclear reprocessing plant after cooling [10]. Regardless, assuming the availability of U-233 in quantities sufficient to mix with Th-232 in a nuclear reactor, it is critical to investigate the main reactivity and safety coefficients when the reactor is fueled with (Th-^{233}U)O_2.

The incorporation of (Th-^{233}U)O_2 in a pressurized water reactor (PWR) such as the AP1000 design is particularly attractive due to the extensive use of these types of reactors [11-12]. The use of (Th-^{233}U)O_2 as a fuel in today's advanced PWRs is an appealing alternative due to the benefits associated with a high conversion rate and the ability to achieve high fuel burnup, which results in more efficient fuel use and less waste. E.g., (Th-^{233}U)O_2 fuel can be proposed to improve the AP1000 reactor's thorium use and proliferation resistance without modifying the conventional fuel assembly. However, as previously demonstrated in some previous research works, using U-233 as a fissile material resulted in an increase in reactivity at the beginning of the cycle (BOC), assuming the same enrichment as U-235 [7-8,13]. To address this issue, an effective burnable absorber (BA) must be loaded to manage the excess reactivity at the BOC. It is also necessary to account for flattening the reactivity curve over time or reducing excess reactivity during assembly life.

The initial excess of reactivity in a PWR can be compensated for by absorbing additives in the fuel. Absorbers (also known as poisons) with a relatively higher absorption cross-section than the used fuel and low absorbing reaction products [14]. However, because most BAs reduce cycle length and discharge burnup, they should be chosen in such a way that their impact on fuel cycle performance is minimal. The assembly loading pattern is also critical in this regard, as is the effect of these absorbers on the main safety coefficients [15]. BAs come in a variety of forms, the most common of which are integral fuel burnable absorbers (IFBAs), discrete burnable poison rods (BPRs), and burnable poison particles (BPPs) [16-18]. IFBAs are neutron-absorbing materials that can be homogeneously incorporated into or coated on fuel rods before they are placed within the fuel assembly. Boron, gadolinium, and erbium are common materials used as BA. Boron is used in BPRs as B_4C-Al_2O_3 and as a zirconium diboride (ZrB_2) coating on fuel rods. Gadolinium and erbium are commonly used in fuel rods as mixed oxides (Gd_2O_3 and Er_2O_3), and Gd_2O_3 is also used as particle lodes within PWR fuel pellets [19-21]. Several absorbers, including PaO_2, Lu_2O_3, Dy_2O_3, and AmO_2, are also proposed as BA [22-23]. Among these, PaO_2 (protactinium oxide) exhibits promising performance by increasing cycle length due to its probability of conversion to U-233 [24-25]. However, unlike boron, gadolinium, and erbium, protactinium is not found in nature, so it must be produced artificially [26].

In this research, DRAGON5 [27] computer code was used to perform a reactivity analysis on a typical AP1000 assembly. The simulations aim to perform a thorough neutronic comparison of (Th-^{233}U)O_2 fuel and UO_2 fuel. These include the infinite multiplication factor, reactivity, discharge burnup, temperature coefficients of reactivity, and boron worth coefficients. Furthermore, the effect of adding ZrB_2, Gd_2O_3, Er_2O_3, or PaO_2 to the IFBAs, whether homogeneously mixed or coated on (Th-^{233}U)O_2 fuel rods, on the reactivity properties is

compared. For a better understanding of the results, the same enrichment level (4.95 wt.% of U-235 or U-233) was used in all assembly models.

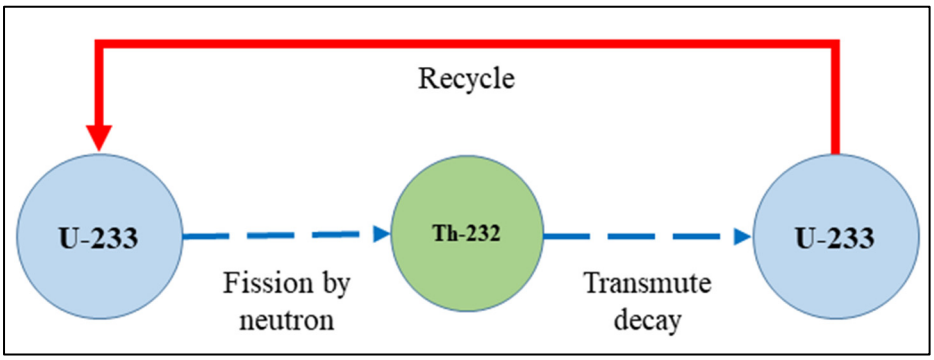

Figure 1. *The ultimate goal of future reactor research is the sustainable use of thorium*

2. Experimental details

2.1. Modeling of the fuel assembly

PWRs are a type of nuclear power reactor that is mostly used for commercial purposes around the world. According to the European Nuclear Society, the global number of operating PWRs has reached approximately 65 percent [28]. Initially designed by Westinghouse Bettis Atomic Power Laboratory for power generation in military ships, PWRs were later developed for commercial use by Westinghouse Nuclear Power Division. The Westinghouse Advanced Passive PWR (AP1000) is a recent PWR development that belongs to the Generation III+ of nuclear reactors [11]. The AP1000 reactor has a capacity of 1117 MWe (3400 MW_{th}). The AP1000 core is composed of 157 fuel assemblies. Each assembly is made up of 264 fuel rods and 25 control rod guide tubes including one central instrumentation tube (waterholes) laid out in a 17 × 17 square array [12, 29]. Tables 1 and 2 highlight the major specifications of the simulated AP-1000 fuel assemblies. Figure 2 depicts a horizontal cutaway view of the DRAGON-modeled AP1000 fuel assemblies fueled by UO_2 and (Th-^{233}U)O_2.

As noted earlier, the use of fissile U-233 my increases the reactivity at the BOC of the PWR assembly operation due to its lower critical mass caused by the higher number of fission neutrons released per neutron absorbed. As a result, to control this excess in reactivity, some rare earth elements with relatively higher neutron absorption, such as gadolinium, need to be used as BA. Boron, gadolinium, and erbium, primarily in the form of ZrB_2, Gd_2O_3, and Er_2O_3, are the most commonly used BA materials in suppressing PWR excess reactivity, particularly at the BOC, due to their large thermal neutron absorption cross-section (Table 3). Recent research studies also show that protactinium-231 in the form of PaO_2 has promising performance because it can lengthen the cycle due to its conversion to U-233. Pa-231 burns more slowly than gadolinium and boron because its neutron absorption cross-section is lower (Table 3). As a result, it does not result in a significant reactivity penalty over the fuel cycle. However, due to residual concentration, a low neutron absorption cross-section causes some reactivity penalty at the end of the cycle (EOC) [30]. In this work, the effect of ZrB_2, Gd_2O_3, Er_2O_3, and PaO_2 on IFBA, whether homogeneously mixed or coated on fuel rods in separate operation cycles, on the reactivity and reactivity coefficients of the AP1000 assembly fueled with (Th-^{233}U)O_2 while maintaining the same enrichment level. The assembly models shown in Figure 3 were established by replacing some of the assembly's fuel rods with IFBA rods; Table 4 shows the ratios and thicknesses used. The goal was to reduce the initial excess reactivity at the BOC and achieve an infinite multiplication factor (K_{INF}) that does not exceed that of the UO2-fueled assembly during burnup.

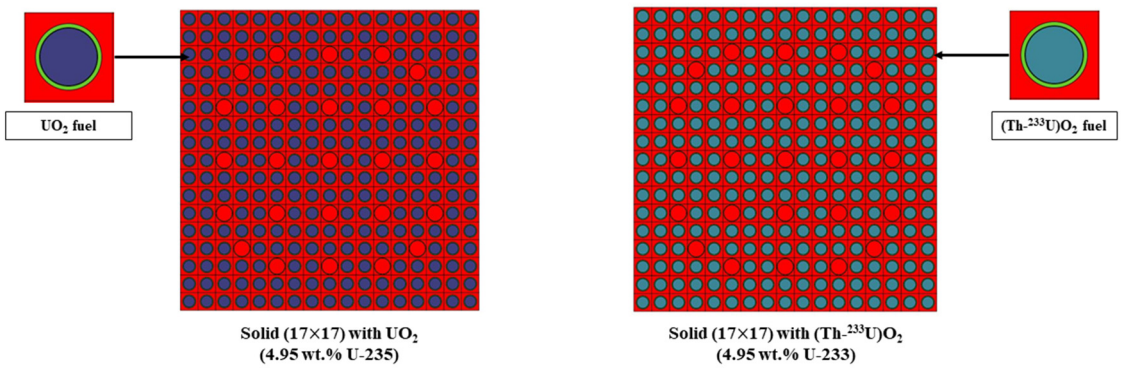

Figure 2. *Horizontal cutaway view of the modeled AP1000 fuel assemblies*

Table 1. *Dimensional specification of fuel rod and guide tube for the studied fuel assembly [12]*

Design Parameters	Values
Rod array	17×17
Number of fuel rods	264
Number of guide tubes	25
Assembly pitch (cm)	21.5
Rod lattice pitch (cm)	1.26
Fuel volume per assembly (cm^3)	5.937E+04
Fuel outer radius (cm)	0.409575
Outer helium gap inner radius (cm)	0.409575
Outer helium gap outer radius (cm)	0.417750
Outer clad inner radius (cm)	0.417750
Outer clad outer radius (cm)	0.474750
Guide tube	
Inner guide tube outer radius (cm)	0.560
Outer guide tube outer radius (cm)	0.600

Table 2. *Data for other assembly properties [12, 31]*

Zone	Parameter	Value
Fuel pellet	UO_2 enrichment	4.95 wt.% (U-235)
	UO_2 density	10.53 g/cm^3
	$(Th\text{-}^{233}U)O_2$ enrichment	4.95 wt.% (U-233)
	$(Th\text{-}^{233}U)O_2$ density	9.95 g/cm^3
Fuel cladding	Cladding material	Zirlo™
	Cladding density	6.50 g/cm^3
Gap	Gap material	Helium
	Gap density at 600 K	1.2049E-02 g/cm^3
	Gap density at 293.6 K	1.6252E-04 g/cm^3
Moderator	Moderator material	Light water
	Moderator density at 600 K	0.711 g/cm^3
	Moderator density at 293.6 K	0.995 g/cm^3
Guide tube cladding	Cladding material	Stainless Steel type 304
	Cladding density	8.03 g/cm^3

Table 3. *Burnable absorbers properties and neutron absorption cross-sections [14, 30]*

BA	Density (g/cm^3)	Melting temperature (°C)	Main absorbing nuclide	Cross-section (Barns)
ZrB_2	6.09	3000	B-10	3844
Gd_2O_3	7.35	2350	Gd-155 Gd-157	60737 252912
Er_2O_3	8.57	2355	Er-167	650
PaO_2	8.90	1572	Pa-231	293

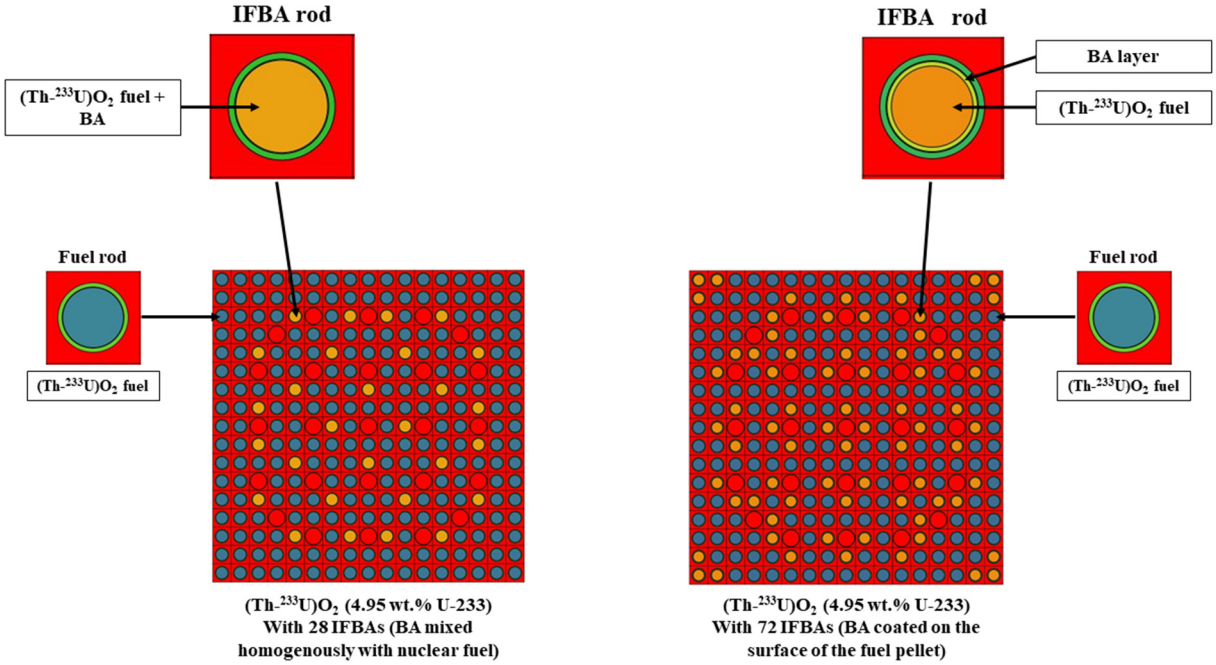

Figure 3. *Horizontal cutaway view of the modeled (Th-^{233}U)O_2 fuel assembly with different cases of BA materials*

Table 4. *Description of assembly designs with BA in IFBAs*

Mixed BA configurations	
(Th-^{233}U)O_2 + 3% ZrB_2	4.95% enriched (Th-^{233}U)O_2 + 28 IFBA rods 3% ZrB_2 mixed
(Th-^{233}U)O_2 + 1% Gd_2O_3	4.95% enriched (Th-^{233}U)O_2 + 28 IFBA rods 1% Gd_2O_3 mixed
(Th-^{233}U)O_2 + 8% Er_2O_3	4.95% enriched (Th-^{233}U)O_2 + 28 IFBA rods 8% Er_2O_3 mixed
(Th-^{233}U)O_2 + 10% PaO_2	4.95% enriched (Th-^{233}U)O_2 + 28 IFBA rods 10% PaO_2 mixed
BA coated in the outer surface configurations	
(Th-^{233}U)O_2 + 0.6 mm ZrB_2	4.95% enriched (Th-^{233}U)O_2 + 72 IFBA rods 0.6 mm coated ZrB_2
(Th-^{233}U)O_2 + 0.6 mm Gd_2O_3	4.95% enriched (Th-^{233}U)O_2 + 72 IFBA rods 0.6 mm coated Gd_2O_3
(Th-^{233}U)O_2 + 2.4 mm Er_2O_3	4.95% enriched (Th-^{233}U)O_2 + 72 IFBA rods 2.4 mm coated Er_2O_3
(Th-^{233}U)O_2 + 3.2 mm PaO_2	4.95% enriched (Th-^{233}U)O_2 + 72 IFBA rods 3.2 mm coated PaO_2

2.2. Computer code

The assembly level calculation presented in this work was performed using DRAGON5 code while considering the ENDFB-VIII.0 (XMAS 172-group) as the cross-sections library source [27]. DRAGON is an open-source simulation package created by Ecole Polytechnique de Montreal in Canada. It is a deterministic neutron transport code for lattice or fuel assembly physic calculations. DRAGON code can solve the Boltzmann neutron transport equation numerically using a variety of methods, including the collision probability method (Pij), the characteristic method (MOC), and the spherical harmonics method (SN). DRAGON can also compute burnup chains for nuclides. Since DRAGON is a modular code, there are many modules available within the code to perform calculations for various lattice geometry such as cartesian square, hexagonal, or cylindrical geometry. Because an AP1000 assembly is based on a square geometry, geometrical modeling was performed in this work by the GEO module using CARCEL-type geometry for cartesian mesh. MESHX and MESHY are used to define the spatial mesh which defines the regions along the X and Y axes. SPLITR is used to specify the geometry's mesh splitting along the radial direction. The EXCELT module, which is based

on the Pij method, tracked the spatial geometry. Tracking performs zone numbering operations, volume, and surface area calculations, and generates the integration lines required for a geometry. In addition, the SHI module, enabling the generalized Stamm'ler method, was activated during cross-section generation to account for the self-shielding effect. The information obtained from this tracking operation was then used in the collision probability calculation performed by the ASM module. The EDI module allows for the averaging and condensing of cross-sections. The EVO module is used for burnup calculations. Furthermore, the boundaries of the fuel assembly are assumed to be reflective. In other words, no neutron leakage is considered [27, 32-33].

2.3. Calculation methodology

The neutronic properties of the AP1000 assemblies studied used reflective boundary conditions. The burnup procedure simulates 1626 Effective Full Power Days (EFPDs), assuming a constant specific power (power per unit fuel mass) of 31.9713 kW/kg during burnup at the Hot Zero Power condition (Fuel, moderator, and structure temperatures were set to 600 K) [12]. Since we are comparing UO_2 and (Th-^{233}U)O_2 fuel in the AP1000 assembly, as well as the effect of using different BAs in (Th-^{233}U)O_2 fuel for reactivity control, the specific power was also assumed to be the same for an adequate comparison. Because the models are assumed to have zero neutron leakage for a reflective boundary condition, the multiplication factor in this scenario is equivalent to K_{INF}. However, because the situation is quite different in the physical world, the simulated values of K_{INF} were used to calculate the corresponding reactivity (ρ) from the following equation [34].

$$\rho = \frac{[K_{INF} - (1 + L)]}{K_{INF}} \tag{1}$$

Where ρ represents the reactivity at a given burnup period for a given neutron leakage fraction L. Different reactor designs have different core neutron leakage fractions. In this study, 4% is used as a typical representative value for a large PWR core like the AP1000 design when 2D lattice-level calculations are used [35].

Temperature coefficients of reactivity, which denote the change in reactivity per degree of temperature change, are another critical reactivity coefficient in reactor design. The fuel temperature coefficient (FTC) and moderator temperature coefficient (MTC) are typically the two dominant temperature reactivity coefficients. In the MTC calculation, the fuel temperature was kept at 600 K, the moderator temperature was lowered to 293.6 K, and the density was increased from 0.711 g/cm^3 to 0.995 g/cm^3. Meanwhile, to calculate the FTC, the fuel temperature was lowered to 293.6 K while the moderator temperature remained at 293.6 K (i.e. Cold Zero Power condition [12]). The temperature coefficients of reactivity (α_T) were calculated using the formula shown in equation (2) [36].

The boron worth coefficient (BW) is also another important reactivity coefficient. For BW calculation, the boron concentration (BC) in the moderator varied between 0 and 2500 ppm, corresponding to the minimum and maximum boron concentration [11], and the reactivity coefficient was calculated using the formula shown in equation (3).

$$\alpha_T = \frac{\Delta\rho}{\Delta T} = \left(\frac{\rho(T) - \rho(T_0)}{T - T_0}\right) * 10^5 [\text{pcm/K}] \tag{2}$$

$$BW = \left(\frac{\Delta\rho}{\Delta BC}\right) * 10^5 [\text{pcm/ppm}] \tag{3}$$

2.4. Model verification

To verify the DRAGON5 code and the assembly model built with it, a square 17×17 fuel assembly fueled with UO_2 (2.35 wt.% U-235) from the literature was simulated for K_{INF} calculation at BOC [11-12]. Table 4 shows the benchmarking results. The results indicate that there is fairly good agreement with the reference values, providing an initial verification of the designed model. The difference in the K_{INF} value between our result and the serpent result is primarily due to the type of code used, as the serpent is a Monte Carlo code, and the difference between our result and Khoshahval results is most likely due to the cross-section library used, as Khoshahval used the IAEA library [33].

Table 4. *Comparison of K_{INF} values for model verification*

Serpent [12]	DRAGON [33]	DRAGON (This work)
1.33112 ± 0.00008	1.316588	1.313455

3. Calculation results and observations

3.1. Evolution of reactivity and achievable discharge burnups

Figure 4(a) illustrates how K_{INF} varies with fuel burnup for UO_2 and (Th-^{233}U)O_2 fuel assemblies. Despite the fact that the two investigated fuel assemblies had the same enrichment of fissile material, the K_{INF} value of (Th- ^{233}U)O_2 was greater than that of UO_2 at the BOC. This is due to the fact that U-233 requires less concentration to achieve the critical condition (Figure 4). Then, in the first stage, the burnup dependent K_{INF} decreases due to fission product poisoning and fuel depletion. Many research studies show that (Th- ^{233}U)O_2 has a low production rate when it comes to fission product poisoning (e.g., Xe-135 and Sm-149) accumulation during the assembly operation [8, 36-37]. Returning to the variation of K_{INF} during burnup, the (Th-^{233}U)O_2 assembly shows a slow decrease rate. This is because variation in U-233 flows a slow depletion rate; this pattern is supported by the conversion of Th-232 to U-233 (Figure 4). As is also known, Th-232 has a larger thermal neutron absorption cross-section than U-238, so the conversion ratio of Th-232 to U-233 is greater than the conversion ratio of U-238 to Pu-239. The reactivity was calculated using the simulated value of K_{INF}, and a comparison at 4% neutron leakage is shown in Figure 4(b). The (Th-^{233}U)O_2 assembly had the least negative value for reactivity at EOC. The (Th-^{233}U)O_2 assembly reaches the critical condition at 1407 EFPDs, whereas the UO_2 assembly reaches the critical condition at 1167 EFPDs.

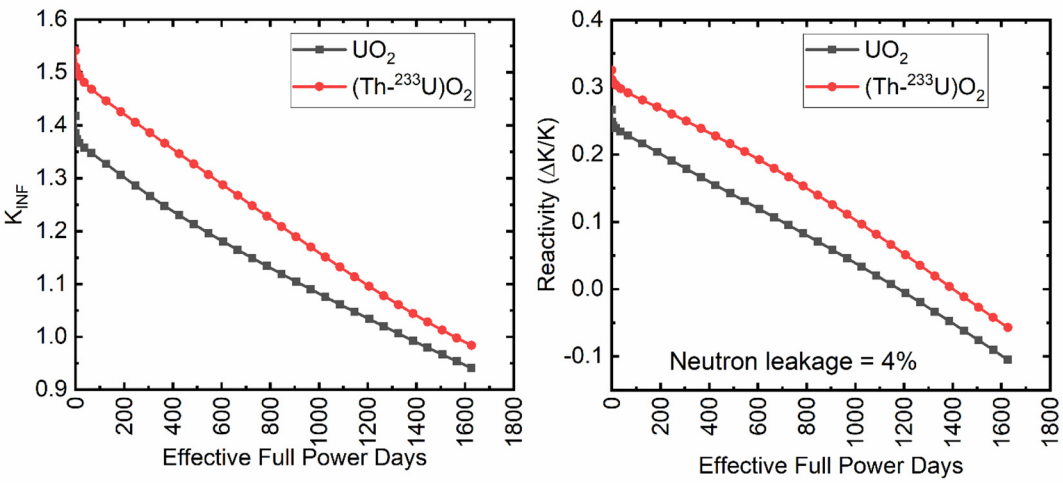

Figure 4. *K_{INF} and reactivity at 4% neutron leakage evolution resulting from assembly calculations performed for UO_2 and (Th-^{233}U)O_2 fuel*

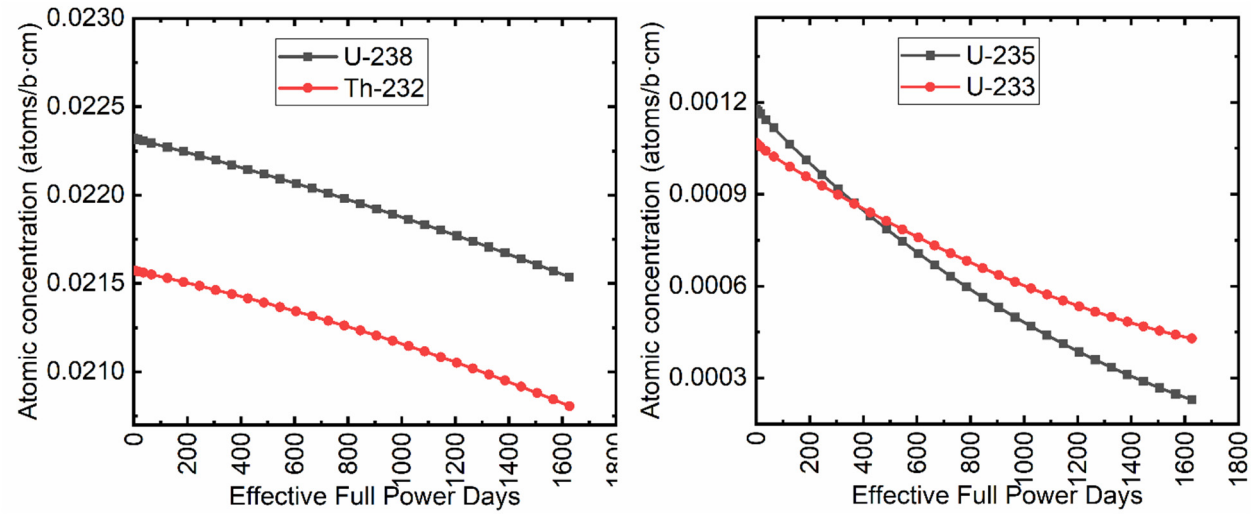

Figure 5. *Comparison of the variation of the used fertile and fissile atomic concentrations with fuel burnup*

3.2. Temperature coefficients of reactivity

As previously discussed, the MTC and FTC are two important coefficients that represent the negative feedback. Inherent safety requires both of these reactivity coefficients to be negative for overall reactor operation because negative coefficients ensure stable reactor operation. Evolutions of the MTC and FTC for UO_2 and (Th-^{233}U)O_2 fuel assembly are compared in Figure 6. The results show that the MTC at BOC for (Th-^{233}U)O_2 assembly is less negative and tends to be positive. In general, increasing the moderator temperature and decreasing its density causes the neutron spectra to harden and shift toward higher neutron energies, resulting in an increase in the fraction of epi-thermal neutrons, a decrease in the fission rate, and an increase in the capture rate, resulting in a decrease in reactivity. The situation with U-233, on the other hand, is exactly the opposite of that with U-235, with the MTC being positive when U-233 is the primary fission source or the dominant fissile. Because fissile U-233 contributes to fission in the epi-thermal range [4][38]. Conversely, Figure 6(b) shows that (Th-^{233}U)O_2 assembly has significantly more negative FTC at BOC than UO_2 assembly because as the fuel temperature rises, the ability of Th-232 to absorb neutrons rises (i.e. due to Doppler Effect [39][40]) while the ability of U-233 to fission decreases (Figure 7). However, during burnup, the masse of Th-232 decreased, contributing to less negative and positive FTC value.

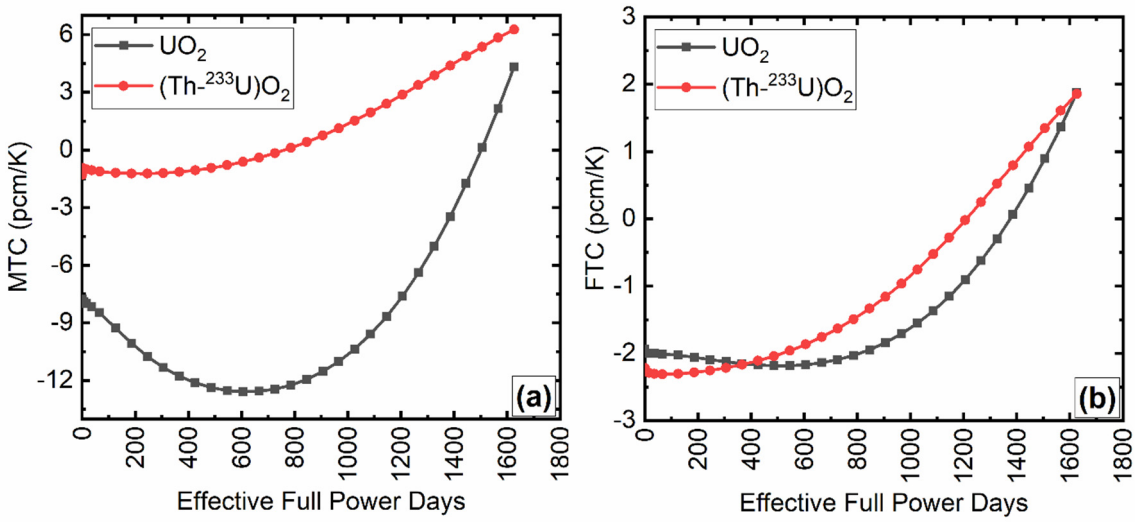

Figure 6. *Burnup-dependent (a) moderator and (b) fuel temperature coefficients*

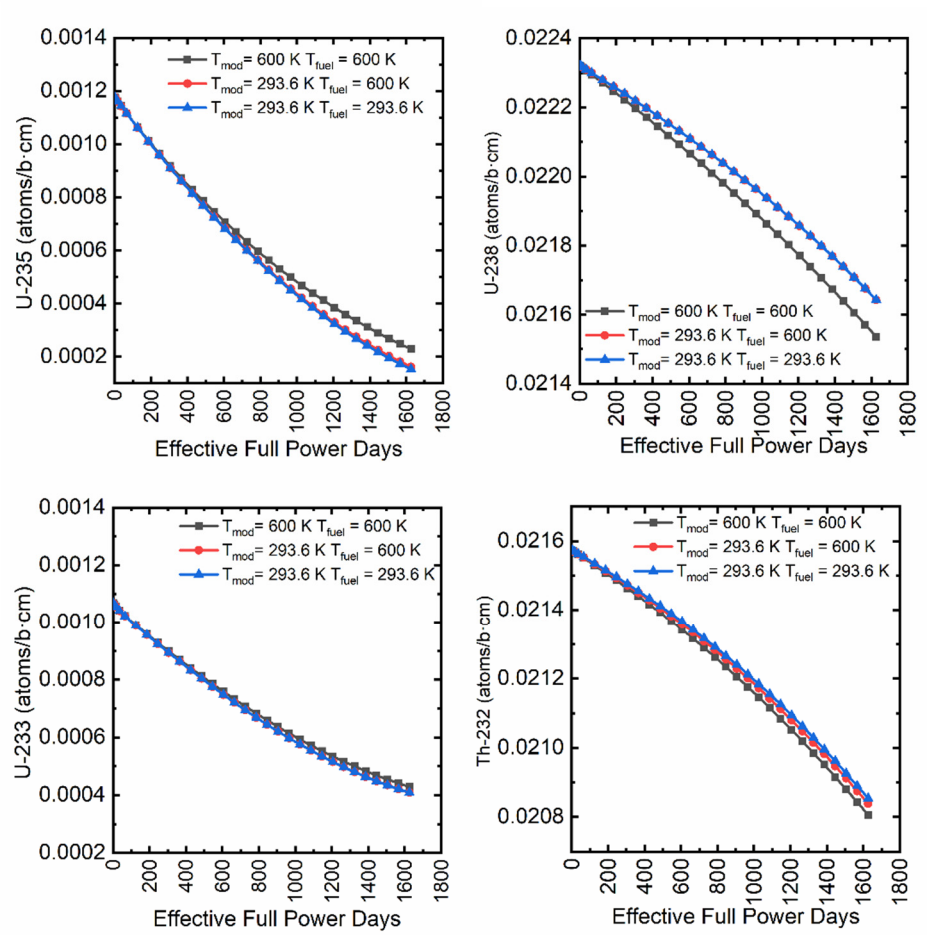

Figure 7. *Evolution of fertile and fissile atomic concentrations in the assemblies studied for the investigated moderator and fuel and temperatures*

3.3. The boron worth coefficient of reactivity

Dissolved boron as BAs is used for initial reactivity suppression, which means providing a poisoning effect. As shown in Figure 8, for both fuel assemblies, the BW calculation results are negative for all given boron concentrations, and the BW coefficient decreases with increasing boron concentration. However, it should be noted that the coefficient is lower in the case of (Th-^{233}U)O_2 assembly and this is mainly due to the presence of U-233.

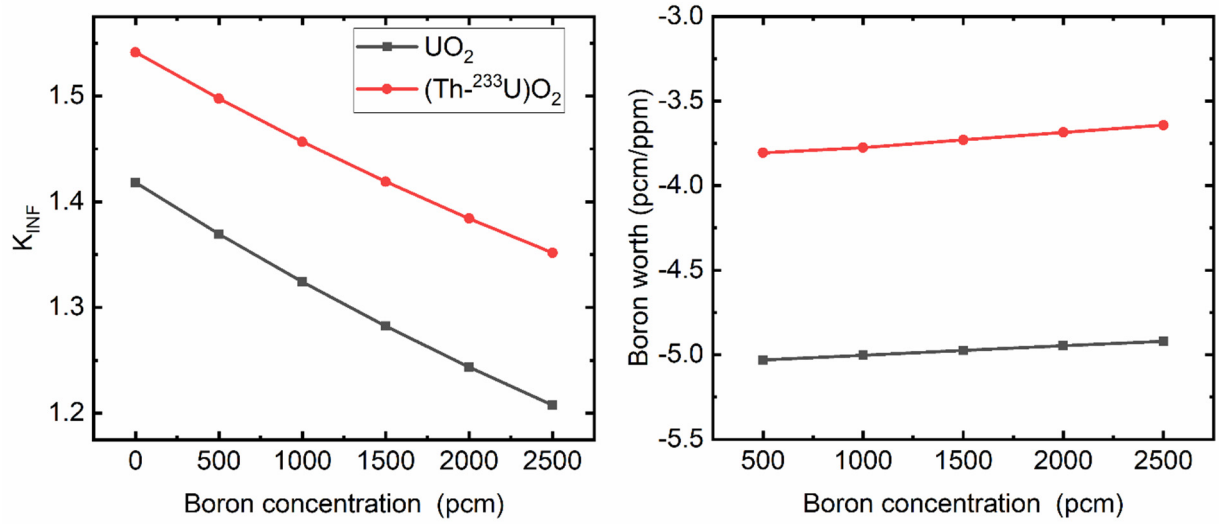

Figure 8. *K_{INF} and boron worth coefficient as a function of boron concentration*

3.4. Evolution of reactivity and achievable discharge burnups using burnable absorbers

The purpose of this section is to assess the effect of using BAs on suppressing reactor reactivity and discharge burnup. Figure 9 shows comparisons between K_{INF} and reactivity at 4% neutron leakage values for various investigated BAs. Figure 9(a) shows mixed BA configurations, and Figure 9(b) shows coated BA configurations. The overall comparison of all proposed configurations and absorbers reveals that adding a BA reduces the reactivity at BOC (Table 5). The thermal utilization factor is reduced when a BA is used in the fuel. The degree of reduction is determined by the absorber's thermal neutron absorption cross-section and concentration. Later, absorber depletion reduces the self-shielding effect, causing the reactivity released during operation. The in-depth comparison reveals that, due to self-shielding effects, the configurations containing absorbers homogeneously mixed inside the rods required a more absorber concentration to achieve a given initial reactivity than the case where the absorber was coated outside the rod (Figure 10). In other words, the allocation of the BA into a larger volume reduces the self-shielding effect.

In terms of cycle length, the behavior of ZrB_2 and Gd_2O_3 with stranger absorption cross-sections is similar. ZrB_2 has the best performance. When compared to non-poisoned (Th-^{233}U)O_2 and UO_2 cycle lengths, the ZrB_2 cases (either mixed or coated) result in the greatest increase in cycle length. The most reactivity flattening occurs in the ZrB_2 cases. While the use of Gd_2O_3 increases reactivity during the cycle due to the fast depletion rate, it also results in the second-largest increase in cycle length. Gd_2O_3 coating has lower reactivity at BOC than a homogeneous Gd_2O_3 mixture, but the end cycle lengths are comparable. In terms of excess reactivity change over the cycle, Er_2O_3 is more effective than Gd_2O_3, but it provided the third-largest increase in cycle length for the homogeneously mixed case and the fourth for the coating case. PaO_2, which has the smallest absorption cross-section when compared to other absorbers, provides the most linear change in reactivity but the least increase in cycle length when compared to UO_2 in the homogeneously mixed case and the third in the coating case. Consequently, using PaO_2 as a coated BA is more efficient than using it in a uniformly mixed configuration. As a result, it can be concluded that BAs with a slow depletion rate results in a smaller increase in the assembly's cycle length. Table 5 shows the assembly's estimated criticality period for each absorber case, based on the time required to achieve zero excess reactivity at 4% neutron leakage.

Although studying the reactivity suppression, swing and cycle length are important parameters, choosing a BA or configuration should also take into account the impact on other safety parameters such as temperature coefficients. Table 6 summarizes the results. The results show a significant difference in behavior between the absorbers studied and the proposed implementation configurations. It can be seen that by using homogeneously mixed IFBA rods, except for Gd_2O_3, the assemblies maintain negative MTCs, and in most cases, those coefficients are more negative than non-poisoned (Th-^{233}U)O_2, especially when using an absorber with a small absorption cross-section, which leads to a higher absorber load. When the temperature of the fuel rises, the FTCs behave similarly to MTCs. All coefficients are negative and higher than the non-poisoned (Th-^{233}U)O_2 assembly, including the Gd_2O_3 assembly, which adds another safety margin. The temperature coefficients of coated IFBA rods behave completely differently than those of homogeneously mixed IFBA rods. The assemblies have relatively negative FTCs, but the MTCs tend to be positive, with the exception of the Er_2O_3 case.

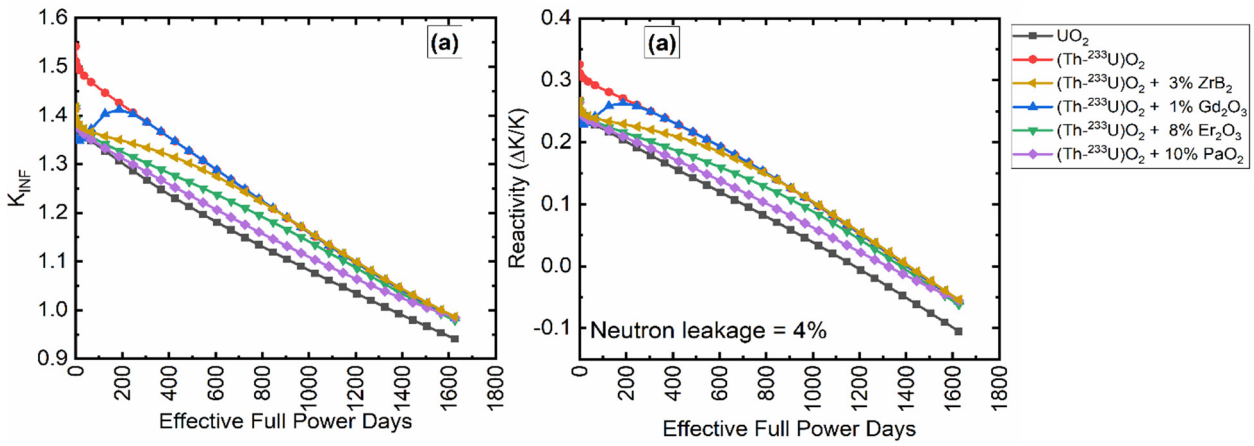

(a)

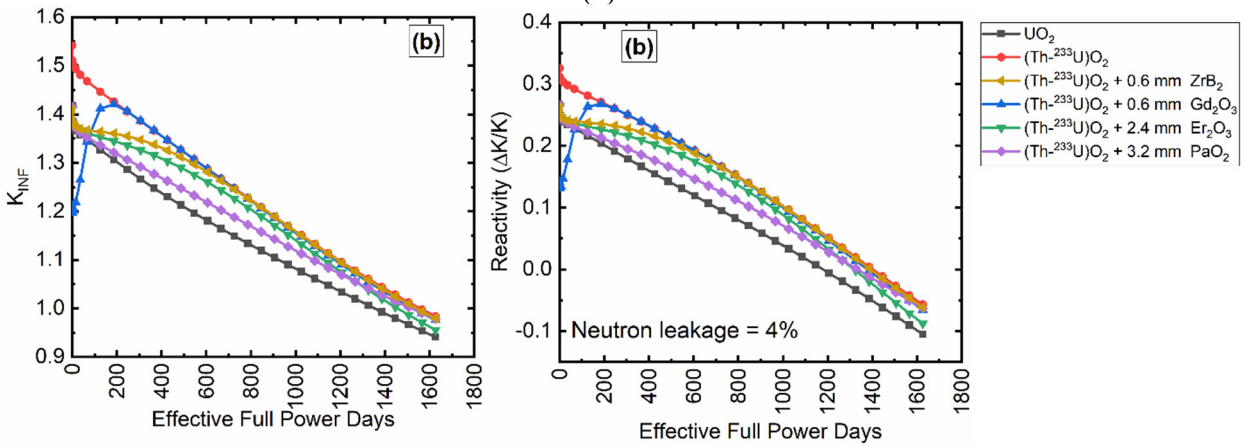

(b)

Figure 9. *Comparison of K_{INF} and the reactivity at 4% neutron leakage for different investigated BAs. (a) mixed configurations. (b) coated configurations*

Table 5. Reactivity at BOC and EOC and the corresponding criticality period at 4% neutron leakage

Assembly compositions	Reactivity at BOC	Reactivity at EOC	Criticality period (EFPDs)
UO_2	0.26671	-0.10511	1167
(Th-^{233}U)O_2	0.32532	-0.05707	1407
(Th-^{233}U)O_2 + 3% ZrB_2	0.26564	-0.05415	1411
(Th-^{233}U)O_2 + 1% Gd_2O_3	0.24282	-0.05660	1392
(Th-^{233}U)O_2 + 8% Er_2O_3	0.26531	-0.06240	1382
(Th-^{233}U)O_2 + 10% PaO_2	0.26440	-0.05568	1323
(Th-^{233}U)O_2 + 0.6 mm ZrB_2	0.26192	-0.06151	1390
(Th-^{233}U)O_2 + 0.6 mm Gd_2O_3	0.14093	-0.06553	1367
(Th-^{233}U)O_2 + 2.4 mm Er_2O_3	0.26417	-0.08799	1283
(Th-^{233}U)O_2 + 3.2 mm PaO_2	0.26507	-0.06280	1333

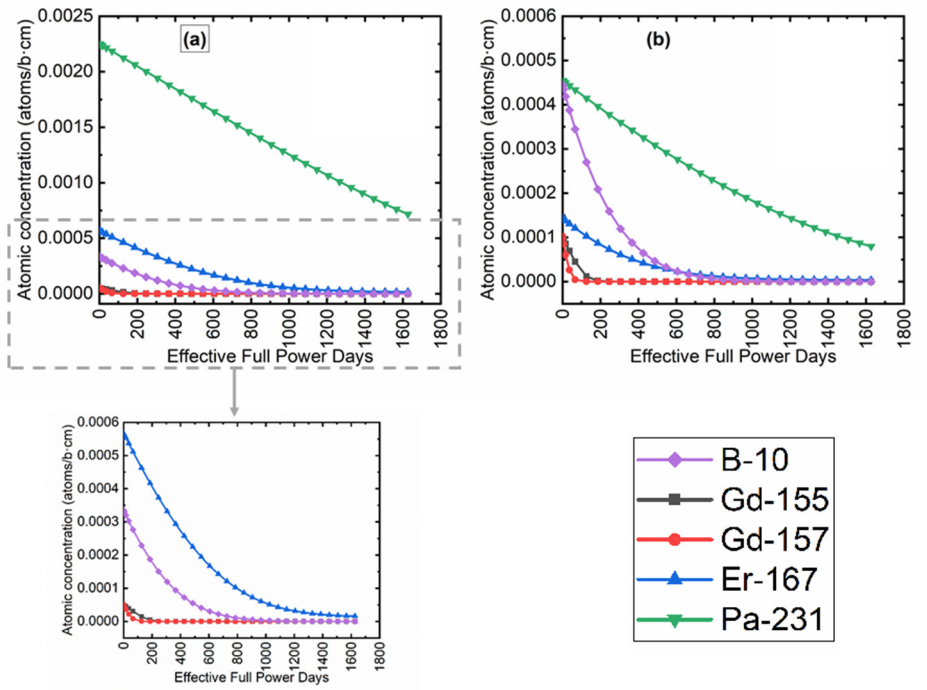

Figure 10. *Variation of atomic concentration of the main absorber isotopes for the analyzed cases with burnup. (a) mixed configurations. (b) coated configurations*

Table 6. *Effect of the addition of BA on MTC and FTC results at BOC*

Assembly compositions	MTC [pcm/K]	FTC [pcm/K]
UO_2	-7.8	-1.9
$(Th\text{-}^{233}U)O_2$	-1.3	-2.2
$(Th\text{-}^{233}U)O_2$ + 3% ZrB_2	-1.3	-2.4
$(Th\text{-}^{233}U)O_2$ + 1% Gd_2O_3	2.1	-2.5
$(Th\text{-}^{233}U)O_2$ + 8% Er_2O_3	-4.3	-2.4
$(Th\text{-}^{233}U)O_2$ + 10% PaO_2	-4.1	-2.6
$(Th\text{-}^{233}U)O_2$ + 0.6 mm ZrB_2	4.8	-2.3
$(Th\text{-}^{233}U)O_2$ + 0.6 mm Gd_2O_3	13.9	-2.7
$(Th\text{-}^{233}U)O_2$ + 2.4 mm Er_2O_3	-1.4	-2.0
$(Th\text{-}^{233}U)O_2$ + 3.2 mm PaO_2	-0.2	-2.0

4. Conclusions

The primary goal of this study was to compare the reactivity coefficients and fuel cycle performance of a $(Th\text{-}^{233}U)O_2$ fueled assembly with and without BAs to the traditional UO_2 assembly design for the AP1000 PWR. Calculations of reactivity change at 4% neutron leakage, MTC, FTC, and BW coefficients were included in the comparisons. The commonly used absorbers include ZrB_2, $Gd2O_3$, and Er_2O_3 as well as PaO_2, which were either homogeneously mixed or coated on $(Th\text{-}^{233}U)O_2$ fuel rods. Several interesting findings have been concluded from the simulation results.

The use of $(Th\text{-}^{233}U)O_2$ fuel with the same UO_2 enrichment results in higher initial excess reactivity and longer cycle length than standard UO_2 fuel due to the highest thermal value of

U-233 and the highest conversion ratio of Th-232 to U-233 during burnup. The FTC and BW are found to be negative for the reactivity control coefficients, while the MTC is found slightly negative and tends to be positive. ZrB_2, Gd_2O_3, Er_2O_3, and PaO_2 were investigated in the IFBA rods of the (Th-^{233}U)O_2 fueled assembly in a separate fuel cycle to suppress the initial excess reactivity and reactivity swing. The addition of a BA (Th-^{233}U)O_2 fuel resulted in an increase in assembly cycle length in all cases considered in the present work when compared to the UO_2 assembly. The ZrB_2, Gd_2O_3, and Er_2O_3 (Er_2O_3 mixed case) cases produced the longest cycle length while maintaining the same excess reactivity as the UO_2 assembly. Except for the ZrB_2 mixed case, the addition of the absorber reduced the assembly cycle length when compared to the non-poisoned (Th-^{233}U)O_2 assembly. PaO_2 coated on IFBA rods outperforms PaO_2 mixed case and Er_2O_3 coated case. As a result, for reactivity control applications, a PWR assembly fueled by (Th-^{233}U)O_2 rods surrounded by PaO_2 layers is preferable. To understand the impact of the addition of BAs on temperature reactivity coefficients, a study of these coefficients has been performed at BOC to examine the impact of both absorber type and the type of implementation. Temperature reactivity coefficients were negative for the mixed cases, except MTC for the Gd_2O_3 case, and in most cases, these coefficients were more negative than those obtained for the non-poisoned (Th-^{233}U)O_2 assembly. The FTCs remain negative in coated cases, but the MTCs become positive. As a result, further optimization of the BA coating would be required to select a specific absorber coating, thickness, and rod locations.

Declaration of competing interest

The authors declare that they have no known competing financial interests or personal relationships that could have appeared to influence the work reported in this paper.

References

[1] K. Insulander Björk, V. Fhager, and C. Demazire, "Comparison of thorium-based fuels with different fissile components in existing boiling water reactors," *Prog. Nucl. Energy*, vol. 53, no. 6, pp. 618–625, 2011.

[2] M. H. Rabir, A. F. Ismail, and M. S. Yahya, "Neutronics calculation of the conceptual TRISO duplex fuel rod design," *Nucl. Mater. Energy*, vol. 27, p. 101005, 2021.

[3] D. Y. Cui *et al.*, "Possible scenarios for the transition to thorium fuel cycle in molten salt reactor by using enriched uranium," *Prog. Nucl. Energy*, vol. 104, pp. 75–84, 2018.

[4] M. H. du Toit and V. V. Naicker, "Neutronic design of homogeneous thorium/uranium fuel for 24 month fuel cycles in the European pressurized reactor using MCNP6," *Nucl. Eng. Des.*, vol. 337, no. July, pp. 394–405, 2018.

[5] A. M. Attom, J. Wang, C. Yan, and M. Ding, "Neutronic analysis of thorium MOX fuel blocks with different driver fuels in advanced block-type HTRs," *Ann. Nucl. Energy*, vol. 129, pp. 101–109, 2019.

[6] D. Baldova, E. Fridman, and E. Shwageraus, "High conversion Th-U233 fuel for current generation of PWRs: Part I – Assembly level analysis," *Ann. Nucl. Energy*, vol. 73, pp. 552–559, Nov. 2014.

[7] O. Kabach, A. Chetaine, A. Benchrif, and H. Amsil, "The use of burnable absorbers integrated into TRISO/QUADRISO particles as a reactivity control method in a pebble-bed HTR reactor fuelled with (Th,233U)O2," *Nucl. Eng. Des.*, vol. 384, no. December, p. 111476, Dec. 2021.

[8] A. A. Galahom, M. Y. M. Mohsen, and N. Amrani, "Explore the possible advantages of using thorium-based fuel in a pressurized water reactor (PWR) Part 1: Neutronic analysis," *Nucl. Eng. Technol.*, no. xxxx, 2021.

[9] M. Lung and O. Gremm, “Perspectives of the thorium fuel cycle,” *Nucl. Eng. Des.*, vol. 180, no. 2, pp. 133–146, 1998.

[10] R. Alvarez, “Managing the Uranium-233 Stockpile of the United States,” *Sci. Glob. Secur.*, vol. 21, no. 1, pp. 53–69, Jan. 2013.

[11] Westinghouse Electric Company LLC, “Chapter 4.3 Nuclear Design AP1000 DCD,” 2004.

[12] G. Laranjo de Stefani, J. M. Losada Moreira, J. R. Maiorino, and P. C. Russo Rossi, “Detailed neutronic calculations of the AP1000 reactor core with the Serpent code,” *Prog. Nucl. Energy*, vol. 116, no. March, pp. 95–107, 2019.

[13] A. Shelley, F. Sharmin, B. Dipa, M. H. Ovi, and M. Salahuddin, “Three-stage fuel option for VVER-1200 reactor,” *Ann. Nucl. Energy*, vol. 171, p. 109025, Jun. 2022.

[14] J. A. Evans, M. D. DeHart, K. D. Weaver, and D. D. Keiser, “Burnable absorbers in nuclear reactors – A review,” *Nucl. Eng. Des.*, vol. 391, no. March, p. 111726, 2022.

[15] U. Mahbuba Nabila and M. Hossain Sahadath, “Neutronic and fuel cycle performance of LEU fuel with different means of excess reactivity control: Impact of neutron leakage and refueling scheme,” *Ann. Nucl. Energy*, vol. 175, p. 109245, Sep. 2022.

[16] H. Yoo, D. H. Hwang, S. G. Hong, and H. C. Shin, “New long-cycle small modular PWR cores using particle type burnable poisons for low boron operation,” *Nucl. Eng. Des.*, vol. 314, pp. 173–181, 2017.

[17] L. Frybortova, “VVER-1000 fuel cycles analysis with different burnable absorbers,” *Nucl. Eng. Des.*, vol. 351, no. May, pp. 167–174, 2019.

[18] H. N. Tran, V. K. Hoang, P. H. Liem, and H. T. P. Hoang, “Neutronics design of VVER-1000 fuel assembly with burnable poison particles,” *Nucl. Eng. Technol.*, vol. 51, no. 7, pp. 1729–1737, 2019.

[19] F. Franceschini and B. Petrović, “Fuel with advanced burnable absorbers design for the IRIS reactor core: Combined Erbia and IFBA,” *Ann. Nucl. Energy*, vol. 36, no. 8, pp. 1201–1207, 2009.

[20] S. Bahauddin Alam, D. Kumar, B. Almutairi, P. K. Bhowmik, C. Goodwin, and G. T. Parks, “Small modular reactor core design for civil marine propulsion using micro-heterogeneous duplex fuel. Part I: Assembly-level analysis,” *Nucl. Eng. Des.*, vol. 346, no. November 2018, pp. 157–175, 2019.

[21] X. H. Nguyen, C. H. Kim, and Y. Kim, “An advanced core design for a soluble-boron-free small modular reactor ATOM with centrally-shielded burnable absorber,” *Nucl. Eng. Technol.*, vol. 51, no. 2, pp. 369–376, 2019.

[22] A. Talamo, “Effects of the burnable poison heterogeneity on the long term control of excess of reactivity,” *Ann. Nucl. Energy*, vol. 33, no. 9, pp. 794–803, 2006.

[23] J. Wang *et al.*, “Multiobjective genetic algorithm strategies for burnable poison design of pressurized water reactor,” *Int. J. Energy Res.*, vol. 45, no. 8, pp. 11930–11942, Jun. 2021.

[24] G. G. Kulikov, A. N. Shmelev, N. I. Geraskin, E. G. Kulikov, and V. A. Apse, “Advanced nuclear fuel cycle for the RF using actinides breeding in thorium blankets of fusion neutron source,” *Nucl. Energy Technol.*, vol. 2, no. 2, pp. 147–150, 2016.

[25] G. G. Kulikov, E. G. Kulikov, A. N. Shmelev, and V. A. Apse, “Protactinium-231 – New burnable neutron absorber,” *Nucl. Energy Technol.*, vol. 3, no. 4, pp. 255–259, 2017.

[26] T. Baatar and E. G. Kulikov, “Justification of VVER-1000 safety when using fuel compositions doped by protactinium and neptunium,” *Nucl. Energy Technol.*, vol. 6, no. 2, pp. 99–104, 2020.

[27] G. Marleau, A. Hebert, R. Roy, and A. Hébert, “A USER GUIDE FOR DRAGON VERSION5,” no. December, 2021.

[28] European Nuclear Society, “Nuclear power plants, world-wide, reactor types,” 2012. [Online]. Available: https://www.euronuclear.org/info/encyclopedia/n/npp-reactor-types.htm. [Accessed: 26-May-2022].

[29] T. L. Schulz, “Westinghouse AP1000 advanced passive plant,” *Nucl. Eng. Des.*, vol. 236, no. 14–16, pp. 1547–1557, 2006.

[30] J. Washington, J. King, and Z. Shayer, “Selection and evaluation of potential burnable absorbers incorporated into modified TRISO particles,” *Nucl. Eng. Des.*, vol. 278, pp. 377–386, 2014.

[31] L. P. Tucker and S. Usman, “Thorium-based mixed oxide fuel in a pressurized water reactor: A burnup analysis with MCNP,” *Ann. Nucl. Energy*, vol. 111, pp. 163–175, Jan. 2018.

[32] M. Paradis, X. Doligez, G. Marleau, M. Ernoult, and N. Thiollière, “ DONJON5/CLASS coupled simulations of MOX/UO 2 heterogeneous PWR core ,” *EPJ Nucl. Sci. Technol.*, vol. 8, p. 4, 2022.

[33] F. Khoshahval, “The effect of enriched gadolinia and its concentrations on the neutronic parameters of AP-1000 fuel assembly,” *Radiat. Phys. Chem.*, vol. 195, no. March, p. 110086, 2022.

[34] M. T. Hossain, M. H. Sahadath, and U. M. Nabila, “Neutronic and fuel cycle performance of VVER-1000 for dual cooled annular fuel with coated burnable poison,” *Prog. Nucl. Energy*, vol. 145, no. September 2021, p. 104139, 2022.

[35] S. B. Alam, C. S. Goodwin, and G. T. Parks, “Parametric neutronics analyses of lattice geometry and coolant candidates for a soluble-boron-free civil marine SMR core using micro-heterogeneous duplex fuel,” *Ann. Nucl. Energy*, vol. 129, pp. 1–12, 2019.

[36] O. Kabach, A. Chetaine, A. Benchrif, H. Amsil, and F. El Banni, “A comparative analysis of the neutronic performance of thorium mixed with uranium or plutonium in a high-temperature pebble-bed reactor,” *Int. J. Energy Res.*, vol. 45, no. 11, pp. 16824–16841, Sep. 2021.

[37] F. El Banni *et al.*, “Neutronic feasibility study of (Th-233U)-Zr H 1.65 fuel in a modelled TRIGA research reactor,” *J. King Saud Univ. - Sci.*, vol. 34, no. 2, p. 101769, Feb. 2022.

[38] N. Deng *et al.*, “Neutronic study of utilization of discrete thorium-uranium fuel pins in CANDU-6 reactor,” *Nucl. Eng. Technol.*, vol. 51, no. 2, pp. 377–383, 2019.

[39] T. Jevremovic, *Nuclear Principles in Engineering*. Boston, MA: Springer US, 2009.

[40] H. K. Joo, J. M. Noh, J. W. Yoo, J. Y. Cho, S. Y. Park, and M. H. Chang, “Alternative applications of homogeneous thoria-urania fuel in light water reactors to enhance the economics of the thorium fuel cycle,” *Nucl. Technol.*, vol. 147, no. 1, pp. 37–52, 2004.